

PAIRING CORRELATIONS IN NUCLEAR SYSTEMS, FROM INFINITE MATTER TO FINITE NUCLEI

Ø. ELGARØY, T. ENGELAND, M. HJORTH-JENSEN AND E. OSNES

Department of Physics, University of Oslo, N-0316 Oslo, Norway

Finite nuclei such as those found in the chain of even tin isotopes from ^{102}Sn to ^{130}Sn , exhibit a near constancy of the $2_1^+ - 0_1^+$ excitation energy, a constancy which can be related to strong pairing correlations and the near degeneracy in energy of the relevant single particle orbits. Large shell-model calculations for these isotopes reveal that the major contribution to pairing correlations in the tin isotopes stems from the 1S_0 partial wave in the nucleon-nucleon interaction. Omitting this partial wave and the 3P_2 wave in the construction of an effective interaction, results in a spectrum which has essentially no correspondence with experiment. These partial wave are also of importance for infinite neutron matter and nuclear matter and give the largest contribution to the pairing interaction and energy gap in neutron star matter.

1 Introduction

One of the fundamental, yet unsolved problems of nuclear theory is to describe the properties of complex nuclei and infinite nuclear matter in terms of their constituent particles and the interaction among them. There are two major obstacles to the solution of this problem. Firstly, we are dealing with a quantal many-body problem which cannot be solved exactly. Secondly, the basic nucleon-nucleon (NN) interaction is not well known. Thus, it may be difficult to know whether an eventual failure to solve this problem should be ascribed to the many-body methods or the interaction model used. On the other hand, these two uncertainties are intimately connected. In any model chosen to approximate the original many-body problem one has to apply an interaction which is consistent with the particular degrees of freedom considered. This amounts to correcting the original interaction for the degrees of freedom not explicitly included in the many-body treatment, thus yielding a so-called effective interaction.

In principle, one should start from an NN interaction derived from the interaction between quarks. Although attempted, this program has not been quantitatively successful. Thus, one has to be content with using an NN interaction derived from meson-exchange models which reproduce the relevant two-nucleon data. Such interactions are generally termed realistic interactions. Once the basic NN interaction has been established, it should be employed in a quantal many-body approximation to the nuclear structure problem of interest. One such approximation is the spherical shell model, which has provided a successful microscopic approach for nuclei near closed shells. In shell-model calculations one typically employs an effective interaction tailored to include those degrees of freedom which are thought to be relevant.

Since the effective interactions employed in shell-model calculations are always the outcome of some truncations in the many-body expansion, the shell model may then provide a useful testing ground for the various approximations made. Furthermore, the shell-model wave function can be used to extract information on

specific correlations in nuclei, such as pairing correlations.

In this study we focus on the link between different partial waves in the NN interaction and the results of large-scale shell-model calculations in the Sn isotopes. We demonstrate that those partial waves which are important for the presence of superfluidity in infinite neutron star matter, play a crucial role in describing the near constancy of the $2_1^+ - 0_1^+$ excitation energy in the chain of even tin isotopes from ^{102}Sn to ^{130}Sn . This near constancy is in turn related to strong pairing correlations.

This contribution falls in four sections. After the above introductory words, we give a brief review of pairing in infinite neutron matter. Shell-model analyses of different approaches to the effective interaction are in turn made in section 3 and concluding remarks are given in section 4.

2 Pairing in infinite neutron matter

The presence of neutron superfluidity in the crust and the inner part of neutron stars are considered well established in the physics of these compact stellar objects. In the low density outer part of a neutron star, the neutron superfluidity is expected mainly in the attractive 1S_0 channel. At higher density, the nuclei in the crust dissolve, and one expects a region consisting of a quantum liquid of neutrons and protons in beta equilibrium. The proton contaminant should be superfluid in the 1S_0 channel, while neutron superfluidity is expected to occur mainly in the coupled $^3P_2 - ^3F_2$ two-neutron channel. In the core of the star any superfluid phase should finally disappear.

The presence of two different superfluid regimes is suggested by the known trend of the nucleon-nucleon (NN) phase shifts in each scattering channel. In both the 1S_0 and $^3P_2 - ^3F_2$ channels the phase shifts indicate that the NN interaction is attractive. In particular for the 1S_0 channel, the occurrence of the well known virtual state in the neutron-neutron channel strongly suggests the possibility of a pairing condensate at low density, while for the $^3P_2 - ^3F_2$ channel the interaction becomes strongly attractive only at higher energy, which therefore suggests a possible pairing condensate in this channel at higher densities. In recent years the BCS gap equation has been solved with realistic interactions, and the results confirm these expectations.

The 1S_0 neutron superfluid is relevant for phenomena that can occur in the inner crust of neutron stars, like the formation of glitches, which may to be related to vortex pinning of the superfluid phase in the solid crust ¹. The results of different groups are in close agreement on the 1S_0 pairing gap values and on its density dependence, which shows a peak value of about 3 MeV at a Fermi momentum close to $k_F \approx 0.8 \text{ fm}^{-1}$ ^{2,3,4,5}. All these calculations adopt the bare NN interaction as the pairing force, and it has been pointed out that the screening by the medium of the interaction could strongly reduce the pairing strength in this channel ^{5,6,7}. However, the issue of the many-body calculation of the pairing effective interaction is a complex one and still far from a satisfactory solution.

The precise knowledge of the $^3P_2 - ^3F_2$ pairing gap is of paramount relevance for, e.g. the cooling of neutron stars, and different values correspond to drastically different scenarios for the cooling process. Generally, the gap suppresses the cooling by

a factor $\sim \exp(-\Delta/T)$ (where Δ is the energy gap) which is severe for temperatures well below the gap energy. Unfortunately, only few and partly contradictory calculations of the pairing gap exist in the literature, even at the level of the bare NN interaction^{8,9,10,11,12}. However, when comparing the results, one should note that the NN interactions used in these calculations are not phase-shift equivalent, i.e. they do not predict exactly the same NN phase shifts. Furthermore, for the interactions used in Refs.^{8,9,10,11} the predicted phase shifts do not agree accurately with modern phase shift analyses, and the fit of the NN data has typically $\chi^2/\text{datum} \approx 3$. Progress has however been made not only in the accuracy and the consistency of the phase-shift analysis, but also in the fit of realistic NN interactions to these data. As a result, several new NN interactions have been constructed which fit the world data for pp and np scattering below 350 MeV with high precision. Potentials like the recent Argonne V_{18} ¹³, the CD-Bonn¹⁴ or the new Nijmegen potentials¹⁵ yield a χ^2/datum of about 1 and may be called phase-shift equivalent. In Table 1 we show the recent non-relativistic pairing gaps for the 3P_2 - 3F_2 partial waves, where effective nucleon masses from the lowest-order Brueckner-Hartree-Fock calculation have been employed, see Ref.¹⁶ for more details. These results are for pure neutron matter and we observe that up to $k_F \sim 2 \text{ fm}^{-1}$, the various potentials give more or less the same pairing gap. Above this Fermi momentum, which corresponds to a lab energy of ~ 350 MeV, the results start to differ. This is simply due to the fact that the potentials are basically fit to reproduce scattering data up to this lab energy. Beyond this energy, the potentials predict rather different phase shifts for the 3P_2 - 3F_2 partial waves, see e.g. Ref.¹⁶. Thus, before a precise calculation of

Table 1. Collection of 3P_2 - 3F_2 energy gaps (in MeV) for the modern potentials discussed. BHF single-particle energies have been used. In case of no results, a vanishing gap was found.

k_F (fm^{-1})	CD-Bonn	V_{18}	Nijm I	Nijm II
1.2	0.04	0.04	0.04	0.04
1.4	0.10	0.10	0.10	0.10
1.6	0.18	0.17	0.18	0.18
1.8	0.25	0.23	0.26	0.26
2.0	0.29	0.22	0.34	0.36
2.2	0.29	0.16	0.40	0.47
2.4	0.27	0.07	0.46	0.67
2.6	0.21		0.47	0.99
2.8	0.17		0.49	1.74
3.0	0.11		0.43	3.14

3P_2 - 3F_2 energy gaps can be made, one needs NN interactions that fit the scattering data up to lab energies of ~ 1 GeV. This means in turn that the interaction models have to account for, due to the opening of inelasticities above 350 MeV, the $N\Delta$ channel.

The reader should however note that the above results are for pure neutron matter. We end therefore this section with a discussion of the pairing gap for β -

stable matter of relevance for the neutron star cooling, see e.g., Ref. ¹⁷. We will also omit a discussion on neutron pairing gaps in the 1S_0 channel, since these appear at densities corresponding to the crust of the neutron star. The gap in the crustal material is unlikely to have any significant effect on cooling processes ¹⁸, though it is expected to be important in the explanation of glitch phenomena. Therefore, the relevant pairing gaps for neutron star cooling should stem from the the proton contaminant in the 1S_0 channel, and superfluid neutrons yielding energy gaps in the coupled 3P_2 - 3F_2 two-neutron channel. If in addition one studies closely the phase shifts for various higher partial waves of the NN interaction, one notices that at the densities which will correspond to the core of the star, any superfluid phase should eventually disappear. This is due to the fact that an attractive NN interaction is needed in order to obtain a positive energy gap.

Since the relevant total baryonic densities for these types of pairing will be higher than the saturation density of nuclear matter, we will account for relativistic effects as well in the calculation of the pairing gaps. As an example, consider the evaluation of the proton 1S_0 pairing gap using a Dirac-Brueckner-Hartree-Fock approach. In Fig. 1 we plot as function of the total baryonic density the pairing gap for protons in the 1S_0 state, together with the results from the non-relativistic approach discussed in Refs. ^{11,19}. These results are all for matter in β -equilibrium. In Fig. 1 we plot also the corresponding relativistic results for the neutron energy gap in the 3P_2 channel. For the 3P_0 and the 1D_2 channels we found both the non-relativistic and the relativistic energy gaps to vanish.

As can be seen from Fig. 1, there are only small differences (except for higher densities) between the non-relativistic and relativistic proton gaps in the 1S_0 wave. This is expected since the proton fractions (and their respective Fermi momenta) are rather small. For neutrons however, the Fermi momenta are larger, and we would expect relativistic effects to be important. At Fermi momenta which correspond to the saturation point of nuclear matter, $k_F = 1.36 \text{ fm}^{-1}$, the lowest relativistic correction to the kinetic energy per particle is of the order of 2 MeV. At densities higher than the saturation point, relativistic effects should be even more important. Since we are dealing with very small proton fractions, a Fermi momentum of $k_F = 1.36 \text{ fm}^{-1}$, would correspond to a total baryonic density $\sim 0.09 \text{ fm}^{-3}$. Thus, at larger densities relativistic effects for neutrons should be important. This is also reflected in Fig. 1 for the pairing gap in the 3P_2 channel. The relativistic 3P_2 gap is less than half the corresponding non-relativistic one, and the density region is also much smaller, see Ref. ¹⁹ for further details.

This discussion can be summarized as follows.

- The 1S_0 proton gap in β -stable matter is $\leq 1 \text{ MeV}$, and if polarization effects were taken into account ⁵, it could be further reduced by a factor 2-3.
- The 3P_2 gap is also small, of the order of $\sim 0.1 \text{ MeV}$ in β -stable matter. If relativistic effects are taken into account, it is almost vanishing. However, there is quite some uncertainty with the value for this pairing gap for densities above $\sim 0.3 \text{ fm}^{-3}$ due to the fact that the NN interactions are not fitted for the corresponding lab energies.
- Higher partial waves give essentially vanishing pairing gaps in β -stable matter.

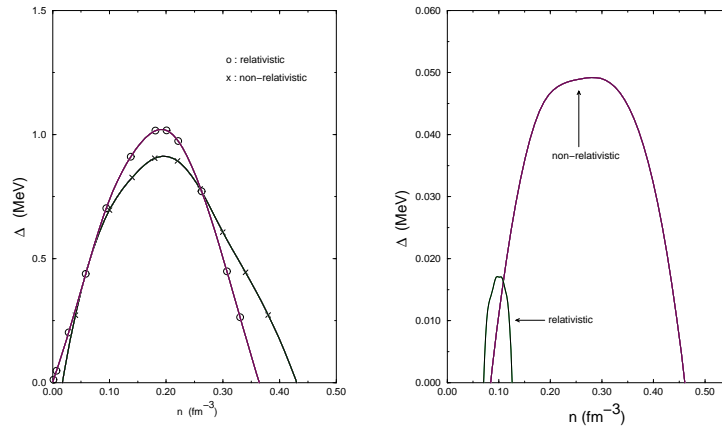


Figure 1. Left box: Proton pairing in β -stable matter for the 1S_0 partial wave. Right box: Neutron pairing in β -stable matter for the 3P_2 partial wave.

Thus, the 1S_0 and 3P_2 partial waves are crucial for our understanding of superfluidity in neutron star matter.

3 Finite nuclei

We turn the attention to finite nuclei. Here we focus on the chain of tin isotopes. Considerable attention is at present being devoted to the experimental and theoretical study of Sn isotopes ^{20,21,22,23,24,25} ranging from the doubly-closed shell nuclei ^{100}Sn to ^{132}Sn . Recently, substantial progress has been made in the spectroscopic approach to the neutron deficient doubly magic ^{100}Sn core. Experimental spectroscopic data are presently available down to ^{102}Sn ²¹. Furthermore, detailed spectroscopy for the other doubly closed-shell nucleus ^{132}Sn have recently been reported by Fogelberg *et al.* ²². Similarly, the experimental single-particle energies of ^{133}Sn have recently been determined ²³. The tin isotopes offer a unique opportunity for examining the microscopic foundation of various phenomenological nuclear models. In the Sn isotopes ranging from mass number $A = 100$ to $A = 132$, neutrons are filling the subshells between the magic numbers 50 and 82, and thus it is possible to examine how well proton-shell closure at mass number 50 is holding up as valence neutrons are being added, how collective features are developing, the importance of certain many-body effects, etc.

Of interest in this study is the fact that the chain of even tin isotopes from ^{102}Sn to ^{130}Sn exhibits a near constancy of the $2_1^+ - 0_1^+$ excitation energy, a constancy which can be related to strong pairing correlations and the near degeneracy in energy of the relevant single particle orbits. As an example, we show the experimental^a $2_1^+ - 0_1^+$ excitation energy from ^{116}Sn to ^{130}Sn in Table 3.1. Our aim is to see whether the partial waves which played such a crucial role in neutron star

^aWe will limit our discussion to even nuclei from ^{116}Sn to ^{130}Sn , since a qualitatively similar picture is obtained from ^{102}Sn to ^{116}Sn .

matter, viz., 1S_0 and 3P_2 , are equally important in reproducing the near constant spacing in the chain of even tin isotopes shown in Table 3.1.

To achieve this, we mount a large-scale shell-model calculation in a model space relevant for the description of tin isotopes. In order to test the dependence on the above partial waves in the NN interaction, different effective interactions are employed.

Our scheme to obtain an effective two-body interaction for the tin isotopes starts with a free nucleon-nucleon interaction V which is appropriate for nuclear physics at low and intermediate energies. In this work we will thus choose to work with the charge-dependent version of the Bonn potential models, see Ref. ¹⁴. The next step in our many-body scheme is to handle the fact that the repulsive core of the nucleon-nucleon potential V is unsuitable for perturbative approaches. This problem is overcome by introducing the reaction matrix G given by the solution of the Bethe-Goldstone equation

$$G = V + V \frac{Q}{\omega - H_0} G, \quad (1)$$

where ω is the unperturbed energy of the interacting nucleons, and H_0 is the unperturbed Hamiltonian. The operator Q , commonly referred to as the Pauli operator, is a projection operator which prevents the interacting nucleons from scattering into states occupied by other nucleons. In diagrammatic language the G -matrix is the sum over all ladder type of diagrams. This sum is meant to renormalize the repulsive short-range part of the interaction. The physical interpretation is that the particles must interact with each other an infinite number of times in order to produce a finite interaction. We calculate G using the double-partitioning scheme discussed in e.g., Ref. ²⁶. A harmonic-oscillator basis was chosen for the single-particle wave functions, with an oscillator energy $\hbar\Omega$ given by $\hbar\Omega = 45A^{-1/3} - 25A^{-2/3} = 7.87$ MeV, $A = 132$ being the mass number.

Finally, we briefly sketch how to calculate an effective two-body interaction for the chosen model space in terms of the G -matrix. Since the G -matrix represents just the summation to all orders of particle-particle ladder diagrams, there are obviously other terms which need to be included in an effective interaction. Long-range effects represented by core-polarization terms are also needed. The first step then is to define the so-called \hat{Q} -box given by

$$P\hat{Q}P = PGP + P \left(G \frac{Q}{\omega - H_0} G + G \frac{Q}{\omega - H_0} G \frac{Q}{\omega - H_0} G + \dots \right) P. \quad (2)$$

The \hat{Q} -box is made up of non-folded diagrams which are irreducible and valence linked. The operator P projects out the two-particle states defined by the model-space. Based on the \hat{Q} -box, we can in turn obtain an effective interaction $H_{\text{eff}} = \tilde{H}_0 + V_{\text{eff}}^{(2)}$ in terms of the \hat{Q} -box, using the folded-diagram expansion, see e.g., Ref. ²⁶ for further details.

The effective two-particle matrix elements are calculated based on a $Z = 50$, $N = 82$ asymmetric core and with the active P -space for holes based on the $2s_{1/2}$, $1d_{5/2}$, $1d_{3/2}$, $0g_{7/2}$ and $0h_{11/2}$ hole orbits. The corresponding single-hole energies are $\varepsilon(d_{3/2}^+) = 0.00$ MeV, $\varepsilon(h_{11/2}^-) = 0.242$ MeV, $\varepsilon(s_{1/2}^+) = 0.332$ MeV,

Table 2. $2_1^+ - 0_1^+$ excitation energy for the even tin isotopes $^{130-116}\text{Sn}$ for various approaches to the effective interaction. See text for further details. Energies are given in MeV.

	^{116}Sn	^{118}Sn	^{120}Sn	^{122}Sn	^{124}Sn	^{126}Sn	^{128}Sn	^{130}Sn
Expt	1.29	1.23	1.17	1.14	1.13	1.14	1.17	1.23
V_{eff}	1.17	1.15	1.14	1.15	1.14	1.21	1.28	1.46
G -matrix	1.14	1.12	1.07	0.99	0.99	0.98	0.98	0.97
1S_0 G -matrix	1.38	1.36	1.34	1.30	1.25	1.21	1.19	1.18

$\varepsilon(d_{5/2}^+) = 1.655$ MeV and $\varepsilon(g_{7/2}^+) = 2.434$ MeV and the shell model calculation amounts to studying valence neutron holes outside this core. The shell model problem requires the solution of a real symmetric $n \times n$ matrix eigenvalue equation

$$\tilde{H} |\Psi_k\rangle = E_k |\Psi_k\rangle. \quad (3)$$

where for the present cases the dimension of the P -space reaches $n \approx 2 \times 10^7$. At present our basic approach in finding solutions to Eq.(3) is the Lanczos algorithm; an iterative method which gives the solution of the lowest eigenstates. This method was already applied to nuclear physics problems by Whitehead *et al.* in 1977. The technique is described in detail in Ref. ²⁷, see also Ref. ²⁴.

3.1 Different approaches to the shell-model effective interaction

In order to test whether the 1S_0 and 3P_2 partial waves are equally important in reproducing the near constant spacing in the chain of even tin isotopes as they are for the superfluid properties of infinite matter, we study four different approximations to the shell-model effective interaction, viz.,

1. Our best approach to the effective interaction, V_{eff} , contains all one-body and two-body diagrams through third order in the G -matrix, see Ref. ²⁵.
2. The effective interaction is given by the G -matrix only and includes all partial waves up to $l = 10$.
3. We define an effective interaction based on a G -matrix which now includes only the 1S_0 partial wave.
4. Finally, we use an effective interaction based on a G -matrix which does not contain the 1S_0 and 3P_2 partial waves, but all other waves up to $l = 10$.

In all four cases the same NN interaction is used, viz., the CD-Bonn interaction described in Ref. ¹⁴. Table 3.1 lists the results obtained for the three first cases.

We note from this Table that the three first cases nearly produce a constant $2_1^+ - 0_1^+$ excitation energy, with our most optimal effective interaction V_{eff} being closest the experimental data. The bare G -matrix interaction, with no folded diagrams as well, results in a slightly more compressed spacing. This is mainly due to the omission of the core-polarization diagrams which typically render the $J = 0$ matrix elements more attractive. Such diagrams are included in V_{eff} . Including only the 1S_0 partial wave in the construction of the G -matrix case 3, yields in turn

Table 3. $2_1^+ - 0_1^+$ excitation energy for the even tin isotopes $^{130-124}\text{Sn}$ obtained with a G -matrix effective interaction which excludes the important pairing waves 1S_0 and 3P_2 . See text for further details. Energies are given in MeV.

	^{124}Sn	^{126}Sn	^{128}Sn	^{130}Sn
No 1S_0 and 3P_2 in G -matrix	0.15	-0.32	0.02	-0.21

a somewhat larger spacing. This can again be understood from the fact that a G -matrix constructed with this partial wave only does not receive contributions from any entirely repulsive partial wave.

It should be noted that our optimal interaction, as demonstrated in Ref. ²⁵, shows a rather good reproduction of the experimental spectra for both even and odd nuclei. Although the approximations made in cases 2 and 3 produce an almost constant $2_1^+ - 0_1^+$ excitation energy, they reproduce poorly the properties of odd nuclei and other excited states in the even Sn isotopes.

However, the fact that the first three approximations result in a such a good reproduction of the $2_1^+ - 0_1^+$ spacing may hint to the fact that the 1S_0 partial wave is of paramount importance. If we now turn the attention to case 4, i.e., we omit the 1S_0 and 3P_2 partial waves in the construction of the G -matrix, the results presented in Table 3.1 exhibit a spectroscopic catastrophe. In this Table we do also not list eigenstates with other quantum numbers. For e.g., ^{126}Sn the ground state is no longer a 0^+ state, rather it carries the quantum numbers 4^+ while for ^{124}Sn the ground state has 6^+ . The first 0^+ state for this nucleus is given at an excitation energy of 0.1 MeV with respect to the 6^+ ground state. The general picture for other eigenstates is that of an extremely poor agreement with data. Since the agreement is so poor, even the qualitative reproduction of the $2_1^+ - 0_1^+$ spacing, we defer from performing time-consuming shell-model calculations for $^{116,118,120,122}\text{Sn}$.

4 Conclusion

In summary, the 1S_0 and 3P_2 partial waves are crucial for our understanding of superfluidity in neutron star matter. In addition, viewing the results of Table 3.1, one sees that pairing correlations, being important for the reproduction of the $2_1^+ - 0_1^+$ excitation energy of the even Sn isotopes, depend strongly on the same partial waves of the NN interaction. Omitting these waves, especially the 1S_0 wave, results in a spectrum which has essentially no correspondence with experiment. Further analyses of the results for finite nuclei will be presented elsewhere ²⁸.

References

1. J.A. Sauls, in: Timing Neutron Stars, eds. H. Ögelman, and E.P.J. van den Heuvel, (Dordrecht, Kluwer, 1989) p. 457.
2. M. Baldo, J. Cugnon, A. Lejeune, and U. Lombardo, Nucl. Phys. **A515**, 409 (1990).
3. V.A. Kodel, V.V. Kodel, and J.W. Clark, Nucl. Phys. **A598**, 390 (1996).

4. Ø. Elgarøy and M. Hjorth-Jensen, Phys. Rev. **C57**, 1174 (1998).
5. H.-J. Schulze, J. Cugnon, A. Lejeune, M. Baldo, and U. Lombardo, Phys. Lett. **B375**, 1 (1996).
6. J.M.C. Chen, J.W. Clark, E. Krotschek and R.A. Smith, Nucl. Phys. **A451**, 509 (1986);
J.M.C. Chen, J.W. Clark, R.D. Dave, and V.V. Khodel, Nucl. Phys. **A555**, 59 (1993).
7. T.L. Ainsworth, J. Wambach, and D. Pines, Phys. Lett. **B222**, 173 (1989); J. Wambach, T.L. Ainsworth, and D. Pines, Nucl. Phys. **A555**, 128 (1993).
8. L. Amundsen and E. Østgaard, Nucl. Phys. **A437**, 487 (1985).
9. M. Baldo, J. Cugnon, A. Lejeune, and U. Lombardo, Nucl. Phys. **A536**, 349 (1992).
10. T. Takatsuka and R. Tamagaki, Prog. Theor. Phys. Suppl. **112**, 27 (1993).
11. Ø. Elgarøy, L. Engvik, M. Hjorth-Jensen, and E. Osnes, Nucl. Phys. **A607**, 425 (1996).
12. V.V. Khodel, PhD. Thesis, Washington University, St. Louis, unpublished (1997); V.A. Khodel, V.V. Khodel, and J.W. Clark, Phys. Rev. Lett. **81**, 3828 (1998).
13. R.B. Wiringa, V.G.J. Stoks, and R. Schiavilla, Phys. Rev. **C51**, 38 (1995).
14. R. Machleidt, F. Sammarruca, and Y. Song, Phys. Rev. C **53**, 1483 (1996).
15. V.G.J. Stoks, R.A. M. Klomp, C.P.F. Terheggen, and J.J. de Swart, Phys. Rev. **C49**, 2950 (1994).
16. M. Baldo, Ø. Elgarøy, L. Engvik, M. Hjorth-Jensen, and H.-J. Schulze, Phys. Rev. **C58**, 1921 (1998).
17. H. Heiselberg and M. Hjorth-Jensen, Phys. Rep., in press and nucl-th/9902033.
18. C.J. Pethick and D.G. Ravenhall, Ann. Rev. Nucl. Part. Sci. **45**, 429 (1995).
19. Ø. Elgarøy, L. Engvik, M. Hjorth-Jensen, and E. Osnes, Nucl. Phys. **A604**, 466 (1996).
20. R. Schneider *et al.*, Zeit. Phys. **A 348**, 241 (1994); Physica Scripta **T56** (1995) 67.
21. H. Grawe *et al.*, Physica Scripta **T56**, 71 (1995); Results presented at Shell 97, Stockholm, 28 october 1997-1 november 1997.
22. B. Fogelberg, M. Hellström, D. Jerrestam, H. Mach, J. Blomqvist, A. Kerek, L. O. Norlin, and J. P. Omtvedt, Phys. Rev. Lett. **73**, 2413 (1994); Physica Scripta **T56**, 79 (1995).
23. P. Hoff *et al.*, Phys. Rev. Lett. **77**, 1020 (1996).
24. T. Engeland, M. Hjorth-Jensen, A. Holt, and E. Osnes, Phys. Scripta **T56**, 58 (1995).
25. A. Holt, T. Engeland, M. Hjorth-Jensen, and E. Osnes, Nucl. Phys. **A634**, 41 (1998).
26. M. Hjorth-Jensen, T. T. S. Kuo, and E. Osnes, Phys. Reports **261**, 125 (1995).
27. R. R. Whitehead, A. Watt, B. J. Cole, and I. Morrison, Adv. Nucl. Phys. **9**, 123 (1977).
28. T. Engeland, M. Hjorth-Jensen, and E. Osnes, in preparation.